

Relaxation and dephasing in a flux qubit

P. Bertet¹, I. Chiorescu^{1*}, G. Burkard², K. Semba^{1,3}, C. J. P. M. Harmans¹, D.P. DiVincenzo², J. E. Mooij¹

¹Quantum Transport Group, Kavli Institute of Nanoscience,

Delft University of Technology, Lorentzweg 1, 2628CJ, Delft, The Netherlands

²IBM T.J. Watson Research Center, P.O. Box 218, Yorktown Heights, NY 10598, USA

³NTT Basic Research Laboratories, Atsugi-shi, Kanagawa 243-0198, Japan

We report detailed measurements of the relaxation and dephasing time in a flux-qubit measured by a switching DC SQUID. We studied their dependence on the two important circuit bias parameters: the externally applied magnetic flux and the bias current through the SQUID in two samples. We demonstrate two complementary strategies to protect the qubit from these decoherence sources. One consists in biasing the qubit so that its resonance frequency is stationary with respect to the control parameters (*optimal point*); the second consists in *decoupling* the qubit from current noise by choosing a proper bias current through the SQUID. At the decoupled optimal point, we measured long spin-echo decay times of up to $4\mu s$.

PACS numbers:

A long-standing problem for the use of superconducting circuits as quantum bits (qubits) in a quantum computer [1, 2, 3, 4] is their relatively short dephasing time compared to the requirements of many-qubit quantum computation. Dephasing is due to the coupling of the qubit's degrees of freedom with the many fluctuating uncontrolled ones commonly denoted as the environment [1, 5]. From the perspective of quantum information, it is crucial to quantitatively identify the various dephasing sources and to find strategies to overcome these, either by reducing the amount of fluctuations or by protecting the qubit against it. An important step in this direction has been accomplished in [3]. The authors showed that dephasing can be significantly reduced by biasing the qubit at an *optimal point* where its resonance frequency is stationary with respect to its control parameters - in that case, gate voltage and magnetic flux.

In this letter we report detailed measurements of the relaxation and dephasing times in a flux-qubit as a function of its bias parameters for two different samples. Our measurements allow us to identify certain dephasing mechanisms and quantify their effect on the qubit. We find that energy relaxation is dominated by spontaneous emission towards the measuring circuit impedance. Dephasing is mainly caused by noise in the external magnetic flux biasing the qubit, thermal fluctuations of our measuring circuit, and low-frequency noise originating from microscopic degrees of freedom, probably causing critical current noise in the qubit junctions. We moreover demonstrate strategies to efficiently fight each of these noise sources.

Our flux-qubit consists of a micron-size superconducting loop intersected with three Josephson junctions [6]. When the total phase across the three junctions γ_Q is close to π , the loop has two low-energy eigenstates (ground state $|0\rangle$ and excited state $|1\rangle$) well separated from the higher-energy ones, which can thus be used as a qubit [4, 7]. The flux-qubit is characterized by two parameters: the minimum energy separation Δ between $|0\rangle$ and $|1\rangle$, and the persistent current I_p . Around

$\gamma_Q = \pi$, the energy separation between these two levels depends on γ_Q and can be written as $E_1 - E_0 \equiv hf_Q = h\sqrt{\Delta^2 + \epsilon^2}$, where $\epsilon \equiv (I_p/e)(\gamma_Q - \pi)/(2\pi)$. The qubit is inductively coupled to a SQUID detector (with a coupling constant M), which is biased at a current I_b . The phase drop γ_Q has two origins: the magnetic flux threading the qubit loop Φ_x , and the currents in the SQUID loop which depend on I_b . Thus, we can write $\epsilon = \eta(\Phi_x) + \lambda(I_b)$.

The coupling of ϵ to fluctuating sources leads to decoherence. Noise in the magnetic flux Φ_x or in the bias current I_b induces fluctuations of the qubit frequency f_Q and thus dephasing. A first strategy to protect the qubit from decoherence consists in biasing it at $\epsilon = 0$ so that $df_Q/d\epsilon = 0$. This is the *optimal point* strategy, which was first invented and demonstrated in [3]. An additional possibility is to *decouple* the external noise from the variable ϵ , by canceling the sensitivity coefficients $d\eta/d\Phi_x$ and $d\lambda/dI_b$. The flux noise can not be decoupled since $d\eta/d\Phi_x = 2I_p/h$ is constant. As we will show below, the bias current noise can be decoupled by biasing the SQUID at a current I_b^* such that $d\lambda/dI_b(I_b^*) = 0$, which is the *decoupling* condition. At the decoupled optimal point, ($\epsilon = 0$ and $I_b = I_b^*$) we expect that the qubit quantum coherence is best preserved, since the qubit is sensitive to flux noise to second order, and to bias current noise to fourth order. We also note that a strong dependence of the dephasing time on the bias current would be clear experimental evidence that current noise, and not flux noise, is the factor limiting the quantum coherence.

In the two samples, shown in figures 1a and 1b, the qubit loop is merged with its measuring SQUID. The dependence of ϵ on the bias current I_b arises from the way this bias current redistributes in the SQUID and eventually generates a phase shift across the qubit junctions via the superconducting line shared by the qubit and the SQUID. The detailed configuration of the shared line is related to the specific fabrication process. We use 2-angle shadow evaporation so that the lines consist effectively of 2 layers. This induces a large asymmetry in the coupling [8] if the qubit loop contains an odd number of junc-

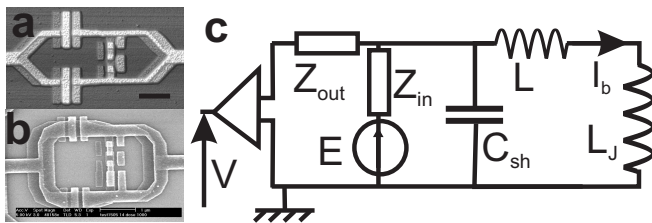


FIG. 1: (a) Atomic Force Micrograph of sample A. The flux qubit is the small loop containing three Josephson junctions in a row ; the SQUID is constituted by the outer loop containing the two large junctions. The bar indicates a $1\mu\text{m}$ length. (b) Scanning Electron Micrograph of sample B. Note that the qubit loop contains a fourth junction, 3 times larger than the other ones. (c) Electrical model of the measuring circuit. The SQUID, represented by its Josephson inductance L_J , is shunted by an on-chip capacitor C_{sh} through superconducting lines of inductance L (all on-chip). It is current-biased by a waveform generator delivering a voltage E across an impedance Z_{in} ; the voltage across the SQUID is connected to the input of a room-temperature preamplifier through an impedance Z_{out} . Z_{in} and Z_{out} include on-chip gold resistors.

tions. In this article, we compare the results obtained for a three- (sample A) and a four- (sample B) junction qubit (see figure 1a and b), and demonstrate that such asymmetry can be removed by using an even number of junctions in the qubit loop [8]. A model for the qubit electromagnetic environment in both samples is shown in figure 1c. The SQUID is modeled by its Josephson inductance L_J shunted by a capacitor C_{sh} via superconducting lines of inductance L . It is connected to the output voltage of our waveform generator E via an impedance Z_{in} , and to the input of a room-temperature amplifier through an impedance Z_{out} . It thus forms a harmonic oscillator, the plasma mode, of frequency $\omega_p = (\sqrt{(L + L_J)C_{sh}})^{-1}$ and quality factor $Q = \omega_p C_{sh} \text{Re}(Z)(\omega_p)$, to which the qubit is strongly coupled [9] (we note $Z = Z_{in}/Z_{out}$). Here is a list of the parameters for our two samples : for sample A, $I_p = 270\text{nA}$, $\Delta = 5.85\text{GHz}$, $M = 20\text{pH}$, $L_J = 80\text{pH}$, $L = 170\text{pH}$, $C = 12\text{pF}$, $Z(0) = 1.4\text{k}\Omega$; for sample B, $I_p = 240\text{nA}$, $\Delta = 5.5\text{GHz}$, $M = 6.5\text{pH}$, $L_J = 380\text{pH}$, $L = 80\text{pH}$, $L_J = 350\text{pH}$, $C = 5.5\text{pF}$, $Z(0) = 9\text{k}\Omega$. We note that the main difference between sample A and B, apart from the number of junctions in the qubit loop, is the value of M and of the low-frequency impedance $Z(0)$.

We measured our sample parameters and $\lambda(I_b)$ by studying the dependence of the qubit Larmor frequency on both the external flux Φ_x and the bias current I_b . We performed spectroscopy by applying a 500ns microwave pulse of variable frequency, and measuring the SQUID switching probability with a short subsequent DC current pulse [4] for different values of Φ_x . We added a $1\mu\text{s}$ plateau at the value I_{bpl} in order to adjust the bias current through the SQUID *during* the application of the microwave pulse. The complete pulse sequence is depicted in figure 2a. In figure 2b the measured qubit res-

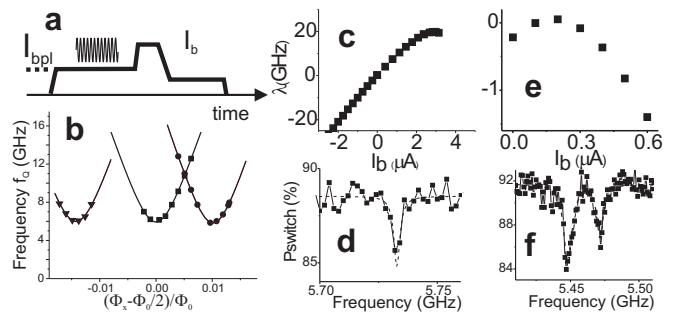


FIG. 2: (a) Principle of the spectroscopy experiments : a bias current pulse of amplitude I_{bpl} (lower than the SQUID critical current) is applied to the sample while a microwave (MW) pulse probes the qubit resonance frequency. The qubit state is finally measured by a short bias current pulse as discussed in [4]. (b) Typical spectroscopy curves for three values of I_{bpl} measured with sample A (from left to right, $I_{bpl} = -2.25, 0, 2\mu\text{A}$). The solid curves are fits to the data. (c,e) Curves $\lambda(I_b)$ deduced from the spectroscopy curves as explained from the text for sample A (c) and sample B (e). The decoupling condition is satisfied at $I_b^* = 2.9 \pm 0.1\mu\text{A}$ for sample A (black arrow in the figure) and $I_b^* = 180 \pm 20\text{nA}$ for sample B. (d,f) Qubit line at the decoupled optimal point for sample A (d) and B (f).

onance frequency for sample A is shown as a function of the external flux Φ_x for three different values of I_{bpl} . We observe that for each value of the bias current, a specific value of external flux $\Phi_x^{(0)}(I_{bpl})$ realizes the optimal point condition.

We fitted all the curves with the formula $f_Q = \sqrt{\Delta^2 + [\lambda(I_b) + 2I_p(\Phi_x - \Phi_0/2)/h]^2}$ for different values of I_b . The obtained curves $\lambda(I_b)$ are shown in figure 2c and 2e for both samples. The decoupling occurs at $I_b^* = 2.9 \pm 0.1\mu\text{A}$ for sample A and at $I_b^* = 180 \pm 20\text{nA}$ for sample B. Note that although the SQUID critical current is similar in both samples, the decoupling current is much closer to 0 in sample B due to the presence of the fourth junction which restores the symmetry of the coupling [8]. We biased our qubit at the decoupled optimal point by setting $I_b = I_b^*$ and $\Phi_x = \Phi_x^{(0)}(I_b^*)$. The qubit line shape under these conditions is shown in figure 2d for sample A and 2f for sample B. For sample A, we could fit it with a Lorentzian of width $w = 3.1 \pm 0.5\text{MHz}$ (FWHM). This width yields a dephasing time $T_2 = 1/\pi w \simeq 100\text{ns}$ consistent with the Ramsey fringe measurements as discussed below. For sample B, the line was split, due to the action of a strongly coupled two-level fluctuator. We fitted it by the sum of two Lorentzians of widths 7 and 6MHz . We note that in addition to the fluctuator responsible for the splitting of the line, the value of the qubit frequency at the optimal point Δ exhibited occasional jumps of around 100MHz . Also the width of the line changed significantly in time. This indicates that dephasing was probably dominated by some low-frequency noise due to one or more strongly coupled microscopic fluctuators, likely generating critical current noise. We

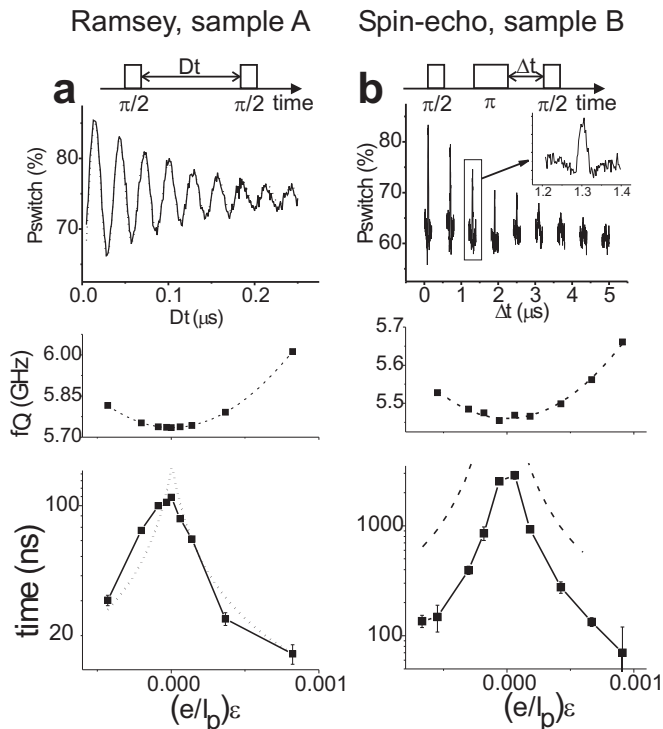


FIG. 3: (a) Ramsey fringe signal measured with sample A. From top to bottom : - temporal sequence of microwave pulses corresponding to a Ramsey experiment. - Ramsey signal at the optimal decoupled point. - Qubit resonance frequency as a function of ϵ . - Dephasing time T_2 as a function of ϵ around the optimal point (full squares, the lines are a guide to the eye), and fit to the data (dotted curve) assuming that dephasing was caused by $1/f$ flux noise $S_{\Phi_x} = 3 \cdot 10^{-12}/f[\Phi_0^2/Hz]$. (b) Spin-echo signal measured with sample B. From top to bottom : Temporal sequence of microwave pulses corresponding to a spin-echo experiment. - Spin-echo signal at the optimal decoupled point. - Qubit resonant frequency as a function of ϵ . - (full squares) : Spin-echo time T_{echo} as a function of ϵ (the lines are a guide to the eye). (dashed curve) : calculated dephasing from thermal fluctuations of the photon number in the SQUID plasma mode.

stress that we had no evidence for such instabilities with sample A.

We first studied the dependence of the dephasing time as a function of ϵ while keeping $I_b = I_b^*$. For sample A, we measured Ramsey fringes [3, 4] by applying a sequence of microwave pulses as schematized in figure 3a for each value of Φ_x . The Ramsey fringes measured at the decoupled optimal point are shown. They decay exponentially with a time constant T_2 . Figure 3a (bottom) shows the dependence of T_2 with Φ_x . The dephasing time exhibits a sharp maximum $T_2 = 120ns$ at the optimal point $\epsilon = 0$ for which $df_Q/d\epsilon = 0$ as expected.

To account for the rapid degradation of the dephasing time when $\epsilon \neq 0$, we first evaluated the effect of the thermal fluctuations in the measuring circuit on the qubit coherence time. Thermal fluctuations of the photon number in the plasma mode cause fluctuations of

the qubit resonance frequency and thus dephasing. It has been shown [14] that treating the thermal fluctuations of the plasma mode as a weak classical perturbation leads to a strong underestimate because of the neglect of quantum correlations between the qubit and the oscillator. Instead, we numerically integrated the master equation for the joint density matrix of the “qubit-plasma mode” system [15]. The qubit density matrix is obtained at the end of the calculation by tracing over the plasma mode degrees of freedom. The evolution of its off-diagonal element yields the dephasing time. For these calculations, we assumed a quality factor $Q = 100$ for sample A and $Q = 150$ for sample B, and an effective temperature $T = 70mK$ in agreement with additional measurements [9]; all the other parameters of the model are directly obtained from experimental data. For sample A, we found that thermal fluctuations have a negligible effect when $I_b = I_b^*$; we thus believe that flux-noise is responsible for rapid degradation of the dephasing time when $\epsilon \neq 0$. Assuming that the flux-noise power spectrum has a frequency dependence given by $S_{\Phi_x} = A/|f|$ which is consistent with noise measurements found in the literature [10], we can use the data from figure 3a to evaluate A . With calculations similar to [12], we find that $A = 3 \pm 1.5 \cdot 10^{-12} \Phi_0^2$ gives a good agreement (dotted line in figure 3a). Such a level of noise is comparable to the lowest values reported in SQUID measurements [10, 11].

As could be expected from the lineshape shown in figure 2f, the Ramsey fringe signal measured with sample B had a non-exponential damping so that it was impossible to measure T_2 . To circumvent the low-frequency noise mentioned above, we used a spin-echo type sequence of microwave pulses shown in figure 3b (top), as demonstrated in the case of low-frequency charge noise [12, 13]. The results are shown in figure 3b at the decoupled optimal point, by a set of curves corresponding to different delays between the two $\pi/2$ pulses. We fitted each curve by a gaussian multiplied by a sine curve. Then we fitted the decay of the echo amplitude as a function of the delay between the two $\pi/2$ pulses with an exponential of time constant T_{echo} . At the decoupled optimal point, we measured $T_{echo} = 3.9 \pm 0.1 \mu s$. We stress that these results represent a significant improvement over previously reported coherence times in superconducting qubits. We studied the dependence of T_{echo} as a function of ϵ (figure 3b bottom, full squares) for $I_b = I_b^*$. Again we found a sharp maximum at $\epsilon = 0$. For sample B, thermal fluctuations in the plasma mode account qualitatively for the experimental data (dashed curve in figure 3b bottom).

We finally studied the bias current I_b dependence of the dephasing and echo times T_2 and T_{echo} together with the energy relaxation time T_1 at $\epsilon = 0$. The results are shown in figure 4a and c for samples A and B respectively. All these curves exhibit a clear maximum at $I_b = I_b^*$. This indicates that at $I_b \neq I_b^*$ both relaxation and dephasing are limited by coupling to the measuring circuit. In particular, the fact that in sample B T_1 is strongly reduced away from I_b^* is a clear indication that energy

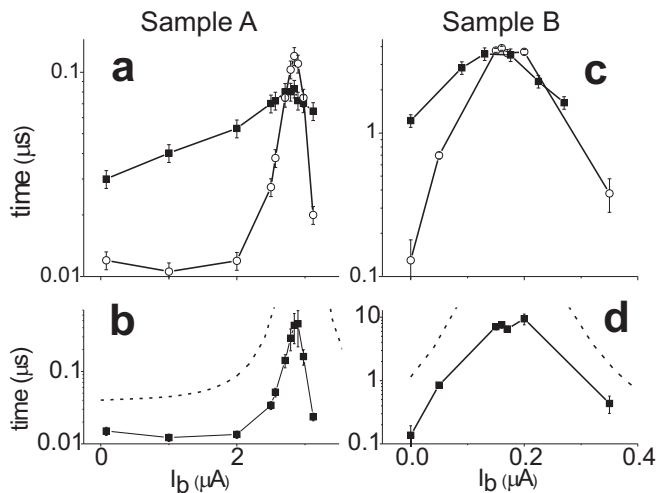


FIG. 4: (a) Relaxation (T_1 , black squares) and dephasing (T_2 , empty circles) times at the optimal point ($\epsilon = 0$) as a function of the bias current I_b for sample A. (b) Pure dephasing time T_ϕ (full squares) as a function of I_b . The dashed line is the result of a simulation taking into account the thermal fluctuations of the plasma mode. (c) Relaxation (T_1 , black squares) and echo (T_2 , empty circles) times at the optimal point ($\epsilon = 0$) as a function of the bias current I_b for sample B. (d) Pure dephasing component of the echo time T_ϕ^{echo} (full squares) and calculated effect of the thermal fluctuations in the plasma mode (dashed line).

relaxation occurs by spontaneous emission towards the circuit impedance seen by the qubit. A weaker dependence is observed for sample A, which could indicate that additional environmental modes at the qubit frequency are involved. The dephasing time T_2 measured in sample A is strongly dependent on I_b . This indicates that dephasing at the optimal point is limited by noise in the bias current. For both samples, the dephasing time

measured at the optimal decoupled point is similar to or larger (sample A) than the relaxation time, so that dephasing was partly limited by relaxation. To quantify the pure dephasing contribution, we calculated T_ϕ defined as $T_\phi^{-1} \equiv (T_2)^{-1} - (2T_1)^{-1}$ for sample A (full square curve in figure 4b) and calculated similarly T_ϕ^{echo} for sample B (full square curve in figure 4b). Our calculations taking into account the thermal fluctuations in the plasma mode are shown as the dashed curve in figures 4b and d. They are in qualitative agreement with the data, although systematically overestimating the dephasing time by a factor typically 5 compared to the measurements.

In conclusion, we presented detailed measurements of the relaxation and dephasing times as a function of bias parameters for two flux-qubit samples. We showed that the *optimal point* concept already demonstrated for the quantum circuit [3] is also valid for the flux-qubit design. Making use of the SQUID geometry of our detector, we could moreover *decouple* the qubit from current fluctuations by biasing the SQUID at a specific current I_b^* . We showed that adding a fourth junction to the qubit loop enhances the symmetry of the coupling, thus lowering the value of I_b^* . We showed that low-frequency noise limits the dephasing time, but that spin-echo techniques provide a powerful tool to fight it. We observed remarkably long decay times of the echo signal of $4\mu\text{s}$, limited by relaxation. We provided quantitative evidence that at the optimal point dephasing is induced by the thermal fluctuations of the photon number in the plasma mode of our SQUID detector. These results indicate that long coherence times can be achieved with flux qubits.

We thank Y. Nakamura, D. Estève, D. Vion, M. Grifoni for fruitful discussions. This work was supported by the Dutch Foundation for Fundamental Research on Matter (FOM), the E.U. Marie Curie and SQUBIT grants, and the U.S. Army Research Office.

-
- [1] Y. Makhlin, G. Schön, and A. Shnirman, *Rev. Mod. Phys.* **73**, 357 (2001).
[2] Y. Nakamura, Yu. A. Pashkin, and J. S. Tsai, *Nature (London)* **398**, 786 (1999) ; J. M. Martinis, S. Nam, J. Aumentado, and C. Urbina, *Phys. Rev. Lett.* **89**, 117901 (2002) ; T. Duty, D. Gunnarsson, K. Bladh, P. Delsing, *Phys. Rev. B* **69**, 140503 (2004) ; J. Claudon, F. Balestro, F. W. Heeking, O. Buisson, *Phys. Rev. Lett.* **93**, 187003 (2004) .
[3] D. Vion et al., *Science* **296**, 886 (2002).
[4] I. Chiorescu, Y. Nakamura, C. J. P. M. Harmans, and J. E. Mooij, *Science* 10.1126/science.1081045 (2003).
[5] E. Paladino, L. Faoro, G. Falci and R. Fazio, *Phys. Rev. Lett.* **88**, 228304 (2002) ; Y. Makhlin, A. Shnirman, *Phys. Rev. Lett.* **92**, 178301 (2004).
[6] J.E. Mooij, T. P. Orlando, L. Levitov, L. Tian, C. H. van der Wal, and S. Lloyd, *Science* **285**, 1036 (1999).
[7] C. H. van der Wal et al., *Science* **290**, 773 (2000).
[8] G. Burkard, D. P. DiVincenzo, P. Bertet, I. Chiorescu, J.E. Mooij, arXiv:cond-mat/0405273 (2004).
[9] I. Chiorescu, P. Bertet, K. Semba, Y. Nakamura, C.J.P.M Harmans, and J.E. Mooij, *Nature* **431**, 159 (2004)
[10] R.H. Koch, J. Clarke, W.M. Goubau, J.M. Martinis, C.M. Pegrum, D.J. van Harlingen, *J. of Low-Temp. Phys.* **51**, 207 (1983).
[11] V. Foglietti, W.J. Gallagher, M.B. Ketchen, A.W. Kleinsasser, R.H. Koch, S.I. Raider, R.L. Sandstrom, *Appl. Phys. Lett.* **49**, 1393 (1986).
[12] Y. Nakamura, Y.A. Pashkin, T. Yamamoto, J.-S. Tsai, *Phys. Rev. Lett.* **88**, 047901 (2002).
[13] E. Collin, G. Ithier, A. Aassime, P. Joyez, D. Vion, and D. Esteve, *Phys. Rev. Lett.* **93**, 157005 (2004).
[14] M. Thorwart, E. Paladino, M. Grifoni, *Chem. Phys.* **296** 333 (2004).
[15] S. Haroche, in “Fundamental Systems in Quantum Optics”, J. Dalibard, J.-M. Raimond, J. Zinn-Justin eds. (Elsevier Amsterdam 1992) p.843.